

2008-01-01

## Method for Characterization of Diffusion Properties of Photopolymerisable Systems

Tzvetanka Babeva

*Technological University Dublin, babeva@gmail.com*

Izabela Naydenova

*Technological University of Dublin, izabela.naydenova@tudublin.ie*

Suzanne Martin

*Technological University of Dublin, suzanne.martin@tudublin.ie*

*See next page for additional authors*

Follow this and additional works at: <https://arrow.tudublin.ie/cieoart>



Part of the [Optics Commons](#)

### Recommended Citation

Babeva, T. et.al. (2008) Method for characterization of diffusion properties of photopolymerisable systems. *Optics Express*, Vol. 16 no. 12, pp.8487-8497. doi:10.1364/OE.16.008487

This Article is brought to you for free and open access by the Centre for Industrial and Engineering Optics at ARROW@TU Dublin. It has been accepted for inclusion in Articles by an authorized administrator of ARROW@TU Dublin. For more information, please contact [arrow.admin@tudublin.ie](mailto:arrow.admin@tudublin.ie), [aisling.coyne@tudublin.ie](mailto:aisling.coyne@tudublin.ie).



This work is licensed under a [Creative Commons Attribution-NonCommercial-Share Alike 4.0 License](#)  
Funder: Science Foundation Ireland

---

**Authors**

Tzvetanka Babeva, Izabela Naydenova, Suzanne Martin, and Vincent Toal

# Method for characterization of diffusion properties of photopolymerisable systems

Tzwetanka Babeva<sup>1\*</sup>, Izabela Naydenova<sup>1</sup>, Suzanne Martin<sup>1</sup>,  
and Vincent Toal<sup>1,2</sup>

<sup>1</sup> Centre for Industrial and Engineering Optics, Dublin Institute of Technology,  
Kevin Street, Dublin 8, Ireland

<sup>2</sup> School of Physics, Dublin Institute of Technology,  
Kevin Street, Dublin 8, Ireland

\*Corresponding author: [tzwetanka.babeva@student.dit.ie](mailto:tzwetanka.babeva@student.dit.ie)

**Abstract:** A novel approach for measuring the diffusion coefficients in photopolymerisable materials is proposed. The method is based on studying the evolution of the surface relief profile in a single illuminated spot using an interferometric surface profiler. It is shown that the observed post-exposure swelling in the illuminated spot is due to mass-transport of monomer from the unexposed to the exposed area driven by a monomer concentration gradient set up by the monomer polymerization in the exposed area. Appropriate choice of the thickness of the studied layers ensures both lateral movement of monomer and negligible contribution from the depth. The diffusion coefficient is retrieved from the standard one-dimensional diffusion equation where the height of the profile in the center of the illuminated spot is used instead of the monomer concentration. In contrast to other techniques for measuring the diffusion in photopolymerisable materials, no assumptions or preliminary information about the polymerization rates are required. It is shown how the method can be used for studying the intensity and polymer density dependence of diffusion coefficient.

© 2008 Optical Society of America

**OCIS Codes:** (160.5470) Polymers; (290.1990) Diffusion; (180.3170) Interference microscopy; (120.6650) Surface measurements, figure; (090.0090) Holography

---

## References and links

1. T. J. Trout, J. J. Schmieg, W. Y. Gambogi, and A. M. Weber, "Optical photopolymers: Design and applications", *Adv. Mat.* **10**, 1219-1224 (1998).
2. A. Sullivan, M. Grabowski, and R. McLeod, "Three-dimensional direct-write lithography into photopolymer", *Appl. Opt.* **46**, 295-301 (2007).
3. S. Guntaka, V. Toal, and S. Martin, "Holographically recorded photopolymer diffractive optical element for holographic and electronic speckle-pattern Interferometry", *Appl. Opt.* **41**, 7475-7479 (2002).
4. H. J. Zhou, V. Morozov, and J. Neff, "Characterization of DuPont photopolymers in infrared light for free-space optical interconnects", *Appl. Opt.* **34**, 7457-7459 (1995).
5. H. Sherif, I. Naydenova, S. Martin, C. McGinn, and V. Toal, "Characterization of an acrylamide-based photopolymer for data storage utilizing holographic angular multiplexing", *J. Opt. A: Pure & Appl. Opt.* **7**, 255-261 (2005).
6. <http://www.inphase-technologies.com/>
7. <http://www.aprilisinc.com/>
8. G. Zhao and P. Mouroulis, "Diffusion model of hologram formation in dry photopolymer materials", *J. Mod. Optics* **41**, 1929-1939 (1994).
9. V. L. Colvin, R. G. Larson, A. L. Harris, and M. L. Schilling, "Quantitative model of volume hologram formation in photopolymers", *J. Appl. Phys.* **81**, 5913-5923 (1997).
10. V. Moreau, Y. Renotte, and Y. Lion, "Characterization of DuPont photopolymer: determination of kinetic parameters in a diffusion model", *Appl. Opt.* **41**, 3427-3435 (2002).

11. S. Piazzola and B. Jenkins, "First-harmonic diffusion model for holographic grating formation in photopolymers", *J. Opt. Soc. Am. B* **17**, 1147-1157 (2000).
12. I. Naydenova, R. Jallapuram, R. Howard, S. Martin, and V. Toal, "Investigation of the Diffusion Processes in a Self-Processing Acrylamide-Based Photopolymer System", *Appl. Opt.* **43**, 2900-2905 (2004).
13. S. Martin, I. Naydenova, R. Jallapuram, R. Howard, and V. Toal, "Two-way diffusion model for the recording mechanism in a self developing dry acrylamide photopolymer", *Proc. SPIE* **6252**, 62525-625217 (2006).
14. S. Martin, C. A. Feely, and V. Toal, "Holographic recording characteristics of an acrylamide-based photopolymer", *Appl. Opt.* **36**, 5757-5768 (1997).
15. A. Havranek, M. Kveton, and J. Havrankova, "Polymer holography II - The theory of hologram growth. Polymer growth detected by holographic method", *Polymer Bulletin* **58**, 261-269 (2007).
16. C. Croutxe-Barghorn and D. J. Lougnot, "Use of self-processing dry photo-polymers for the generation of relief optical elements: a photochemical study", *Pure Appl. Opt.* **5**, 811-827 (1996).
17. J. Neumann, K. S. Wiekling, and D. Kip, "Direct laser writing of surface reliefs in dry, self-developing photopolymer films", *Appl. Opt.* **38**, 5418-5421 (1999).
18. I. Naydenova, E. Mihaylova, S. Martin, and V. Toal, "Holographic patterning of acrylamide-based photopolymer surface", *Optics Express* **13**, 4878-4889 (2005).
19. K. Pavani, I. Naydenova, S. Martin and V. Toal, "Photoinduced surface relief studies in an acrylamide-based photopolymer", *J. Opt. A: Pure Appl. Opt.* **9**, 43-48 (2007).
20. W. J. Roff and J. R. Scott, *Fibers, films, plastics and rubbers, a handbook of common polymers*, (Butterworths, London, 1971).
21. A. Veniaminov and E. Bartsch, "Diffusional enhancement of holograms: phenanthrenequinone in polycarbonate", *J. Opt. A: Pure Appl. Opt.* **4**, 387-392 (2002).
22. R. Jallapuram, I. Naydenova, H. J. Byrne, S. Martin, R. Howard and V. Toal, "Raman spectroscopy for the characterization of the polymerization rate in an acrylamide-based photopolymer", *Appl. Opt.* **47**, 206-212 (2008).
23. S. Gallego, M. Ortuño, C. Neipp, A. Márquez, A. Beléndez, I. Pascual, J. V. Kelly and J. Sheridan, "3 Dimensional analysis of holographic photopolymers based memories", *Optics Express* **13**, 3543-3557 (2005).
24. S. Gallego, C. Neipp, M. Ortuño, A. Beléndez, E. Fernandez and I. Pascual, "Analysis of monomer diffusion in depth in photopolymer materials", *Opt. Commun.* **274**, 43-49 (2007).
25. P. Munk and T. M. Aminabhavi, *Introduction to macromolecular science*, (Jonh Wiley & Sons, Inc., New York, 2002).
26. M. Toishi, T. Tanaka and K. Watanabe, "Analysis of temperature change effects on hologram recording and a compensation method", *Optical Review* **15**, 1-8 (2008).

## 1. Introduction

Interest in photopolymer systems has markedly increased in the past few years for applications in holography [1], manufacturing of optical elements [2,3], optical interconnections [4], holographic data storage [5-7] etc. The demand for further improvement of photopolymer recording capabilities requires deeper understanding of the nature of the recording process. Although the mechanism is rather complicated, it is known that the polymerization and monomer diffusion are the two main processes involved in hologram formation [8]. The monomer diffusion rate is a crucial factor that controls both the recording dynamics and final properties of the holograms [9-11]. Additionally, because monomer diffusion is primarily responsible for the self-developing mechanism, which is regarded as one of the main advantages of the photopolymers, determination of diffusion coefficients is a topic of great importance. However, accurate characterisation of the diffusion coefficients is complicated by continuous changes of polymer density during holographic recording. More precise and unambiguous results can be expected if polymerization and diffusion processes are characterized separately. A previously used approach is the recording of weak holographic gratings with low diffraction efficiency using short exposure times and studying the post-exposure dynamics of the grating's diffraction efficiency [9,12,13]. Even though accurate values may be obtained by holographic measurements it would be a clear advantage to have an independent method for direct measurements of diffusion processes. Therefore, in this

work, instead of measuring the post-exposure diffraction efficiency of the gratings, we studied the post-exposure surface relief profile formation and evolution in a single illuminated spot, using a conventional interferometric profiler. The obtained time and spatial dependences of the profile were used for determination of diffusion coefficient.

## 2. Experimental details

The investigations were performed using a photopolymer system, developed in the Centre for Industrial and Engineering Optics, Dublin Institute of Technology [14], which consists of 17.5 ml stock solution of polyvinyl alcohol (10 w/w%), 2ml triethanolamine, 0.6g acrylamide, 0.2g N,N-methylene bisacrylamide and 4ml Erythrosin B dye (1.1 mM). An amount of 0.4ml of the well mixed solution was gravity settled on a levelled 2.5 cm x 7.5 cm single glass substrate, so the upper surface of the layer was open to the air. The thickness of the layers after drying for 24h in darkness under normal laboratory conditions ( $t^{\circ}=21-23^{\circ}\text{C}$  and 40-60% relative humidity) was about 35  $\mu\text{m}$ .

The illumination of the samples and collection of the surface profiles were performed by White Light Interferometric (WLI) surface profiler MicroXAM S/N 8038. The investigated sample was put with the open surface toward the profiler objective and both the illumination and measurements were performed without moving the sample. The sequence of the measurements in a typical experiment was as follows. Firstly, the image of the unexposed surface was collected. This image was used as a reference to be subtracted from all other images. Then the build-in diaphragm of the WLI profiler (1mm in diameter, positioned 220mm from the sample) was imaged onto the sample surface for 30 s with light of wavelength 554 nm and controlled intensity resulting in an approximately circular spot 55 $\mu\text{m}$  in diameter (Fig. 1a). Finally the exposure was stopped and the images of the sample surface were collected in the dark starting immediately following the exposure. The delivered exposure at one measurement amounts 1/12 of the initial exposure but for estimating its influence on possible changes in the sample it is very important the decrease in sample absorption due to dye bleaching process to be considered. Our measurements have shown that at the end of the illumination the sample absorption decreases from 4 to 50 time compared to initial absorption depending on the used intensity of illumination (5 and 10mW/cm<sup>2</sup>, respectively). Having in mind that 1/12 of the initial exposure is delivered at one measurements the amount of absorbed energy during the measurement will be between 1/48 and 1/600 of the absorption during the initial exposure. Therefore, we can assume that the process of obtaining the profile did not change the sample substantially and did not cause further polymerization.

## 3. Results and discussion

Figs. 1b and 1c present perspective (3D) view and top-view images of the surface, respectively, 45 s after the light is turned off. The vertical and lateral resolutions of the WLI profiler are 1nm and 1 $\mu\text{m}$ , respectively.

To ensure that some of the features in the observed picture are not a result of diffraction from the circular diaphragm we calculated the positions of the characteristic rings of the Airy diffraction pattern. The calculations showed that for diaphragm of 1.0 mm in diameter positioned 220 mm apart from the observation plane the first minimum and maximum of diffraction pattern are expected to appear at distances of about 150  $\mu\text{m}$  and 200  $\mu\text{m}$ , respectively, apart from the image center. This means that a central spot with approximate diameter of 300  $\mu\text{m}$  should be observed if diffraction exists. From the top-view image fig. 1c it is seen that the spot diameter is approximately 55  $\mu\text{m}$ , so the spot is almost 6 time smaller than it should be if it is a result from diffraction effects. Therefore, we can neglect possible

spatial variations of the intensity in the spot arising from diffraction and assume that the spot is almost homogeneously illuminated.

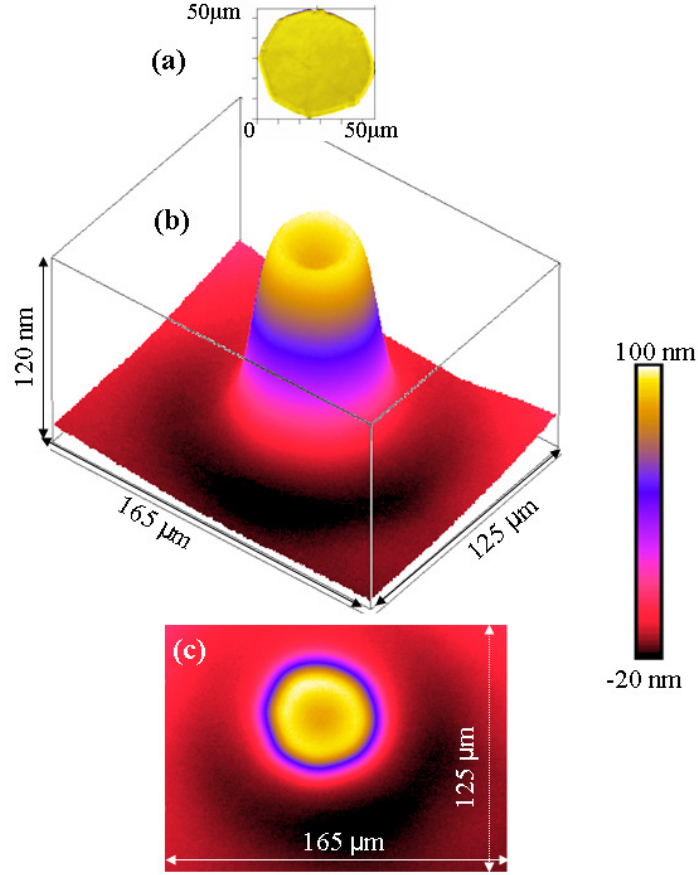


Fig. 1. (Color online) Typical images of the aperture (a) and the surface relief profile-perspective (b) and top view (c) collected by WLI.

Fig. 2a presents the post-exposure time evolution of the cross-section of the profile for initial illumination with intensity of  $10\text{mW}/\text{cm}^2$  for a time of 30s. The post-exposure time dependence of the profile height at the centre of the spot is presented in Fig. 2b where  $t=0$  is defined as the time at the end of the exposure.

Having in mind both that WLI converts measured phase shift data into a topographical map of the surface and that there are two contributors to phase change - refractive index and surface shape changes, ( $\Delta n$  and  $\Delta h$ , respectively) the first issue that should be addressed concerns the origin of the observed profile changes. In the case of normal light incidence the overall phase change  $\Delta\varphi$  initiated by refractive index and surface shape variation ( $\Delta n$  and  $\Delta h$ ) can be estimated from the expression:

$$\Delta\varphi = \Delta\varphi_n + \Delta\varphi_h = \frac{\partial\varphi}{\partial n} \Delta n + \frac{\partial\varphi}{\partial h} \Delta h = \frac{2\pi}{\lambda} (h\Delta n + n\Delta h), \quad (1)$$

where  $\lambda$  is the wavelength of light and  $\Delta\varphi_n$  and  $\Delta\varphi_h$  are the phase change contributions of refractive index  $n$  and surface height  $h$ , respectively. Therefore the ratio of the influences of  $n$  and  $h$  on  $\Delta\varphi$  can be estimated from:

$$\frac{\Delta\varphi_h}{\Delta\varphi_n} = \frac{n\Delta h}{h\Delta n} = \frac{\Delta h/h}{\Delta n/n}. \quad (2)$$

If  $n$  of the polymer layer is about 1.5, for  $\Delta n/n$  we obtain a value of about  $7 \times 10^{-5}$  assuming that in the case of short exposure the refractive index change is approximately  $10^{-4}$  [12,13].

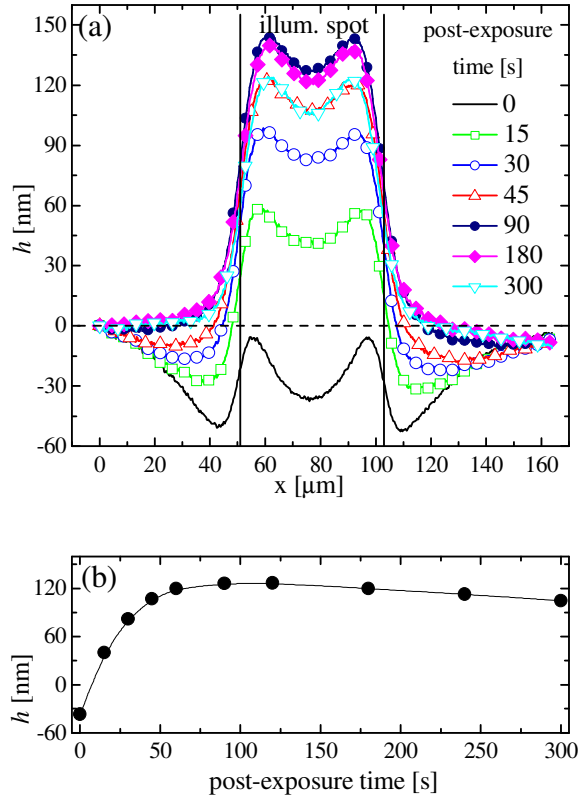


Fig. 2. (Color online) a) Cross-sections of the post-exposure time evolution of the surface relief profile. The unexposed sample surface is indicated by horizontal dashed line. Vertical solid lines mark the illuminated spot; b) Time dependence of the profile center height ( $t=0$  is the time when exposure was stopped) (initial exposure of 30s with intensity of  $10 \text{ mW/cm}^2$ )

From Fig. 2b it is seen that in the time interval  $t=0-15\text{s}$   $\Delta h=77\text{nm}$  and  $h=37\text{nm}$ , so  $\Delta h/h=1.9$  and decreases to about  $8 \cdot 10^{-3}$  for  $t=90-120\text{s}$  ( $\Delta h=1\text{nm}$ ,  $h=127\text{nm}$ ). The ratio between  $\Delta\varphi_h$  and  $\Delta\varphi_n$  calculated from Eq. (2) changes from about  $2.7 \times 10^4$  to 110. Consequently, in the worst case, the phase change contribution of the height of the surface profile is about 110 times greater than the refractive index contribution. This leads to the conclusion that the observed profile changes are mainly due to shape changes.

### 3.1 Surface relief profile evolution

Figure 2a shows that the exposure initiates shrinkage of the sample due to the polymerization. It is seen that after the exposure (the black solid line without markers) the surface relief profile is below the unexposed sample surface indicated by the horizontal dashed line. The faster consumption of the monomer in the illuminated area sets up a concentration gradient and monomer starts to diffuse from the unexposed to the exposed area. Even after exposure the gradient continues to drive monomer diffusion and the surface relief profile continues to grow. After some time, depending on the conditions of the initial illumination, a decrease in profile height is detected. Similar processes (giving rise to an initial increase followed by a decrease in diffraction efficiency) were observed in the post-exposure dynamics of the holographic gratings recorded with short exposure times [9,12,13]. The processes were distinguished as monomer and short polymer chain diffusion processes in opposite directions and quantified [12,13,15]. Considering the analogy between the post exposure dynamics of weak gratings and post exposure profile development in a single illuminated spot we assume that the primary reason for the observed swelling of material in the illuminated spot is the mass transport of monomer from the dark to bright area driven by the concentration gradient. This assumption is also consistent with the explanation of the surface relief grating formation during holographic recording reported in the literature [16, 17]. Furthermore, the swelling in the illuminated area is observed routinely in gratings recorded in this material and has been investigated in detail elsewhere [18, 19].

Nevertheless, to verify the assumption we carried out two control experiments. Firstly in order to check if there is some thermal expansion of the surface we studied monomer-free samples. We could rule out polymerisation caused expansion of monomer containing samples, because it is known that acrylamide shrinks during polymerization [14]. The measurements were performed as described above. The results showed that the surface profile changes in monomer-free samples were negligible, typically 1-2 nm in height. The rough estimations that we have made for expected increase of temperature and consequent thermal expansion of the PVA layer showed that the exposure with 5mW/cm<sup>2</sup> intensity for 30 s leads to increase of temperature in the layer by ten degrees resulting in thermal expansion of 40 nm. Because the transmittance of the layers at 554nm is about 60%, in the calculations we assumed that 40% of the incident energy is absorbed and transformed into heat. The values of specific heat capacity of 1650 Jkg<sup>-1</sup>K<sup>-1</sup>, density of 1200 kgm<sup>-3</sup> and linear thermal expansion of 10<sup>-4</sup> K<sup>-1</sup> [20] are used in the calculations. The higher values of calculated thermal expansion as compared to the measured showed that the amount of energy that is transformed into heat is less than we have assumed. This can be explained with the decrease of the sensitizing dye absorption with time that will lead to decrease in absorbed energy with time. Further, considering both that for monomer-containing samples the surface changes about by 120nm (Fig.2) and that the surface does not change for monomer-free samples we can conclude that the movement of monomer is responsible for the swelling in the illuminated area.

Secondly to check if the observed swelling is due to monomer diffusion we studied the surface relief profile using spots with different sizes (55, 75 and 100 μm) obtained by adjusting the WLI diaphragm. Increasing the size of the spot keeping the same conditions of initial illumination will increase the distance over which the monomer should diffuse in order to reach the center of the spot. So, the time required for monomer to diffuse from non-illuminated area to the center of the illuminated spot will increase. If  $r$  is the radius of the spot and  $D$  and  $\tau$  are diffusion coefficient and diffusion time,  $\tau$  should be expected to increase linearly with square of the spot radius [10,11]:

$$r^2 = 2D\tau. \quad (3)$$



Fig. 3 presents the post-exposure temporal evolution of the profile height at the center of each spot after initial illumination for 30s with intensity of 10 mW/cm<sup>2</sup> (again the point  $t=0$  was the time when exposure was stopped).

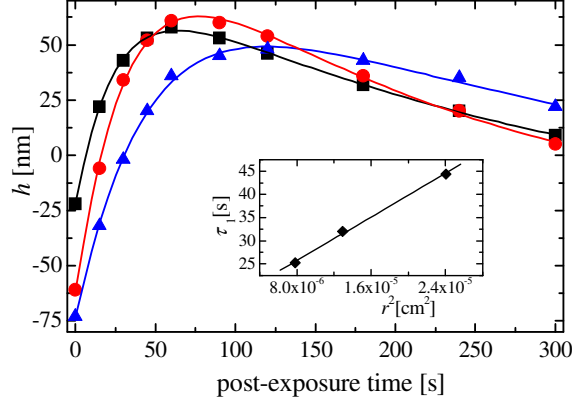


Fig. 3. (Color online) Exponential fit of the post-exposure time dependence of the profile height at the center of the spots with different diameters: 50 $\mu$ m (squares), 75 $\mu$ m (circles) and 100 $\mu$ m (triangles). Inset: the calculated time constant  $\tau_1$  (Eq. (4)) as a function of squared spot radius. (Initial illumination for 30s with 10mW/cm<sup>2</sup>)

A clear dependence of the temporal curves on spot diameter can be seen. The diffusion times could be extracted from the bi-exponential fit of each experimental curve [9,12,13]. For systems with heterogeneity of diffusing species (presence of two monomers and different length polymeric chains in our case) the stretch exponential function is more suitable than a single exponent [13,21]:

$$h = A_1 \exp\left[-\left(\frac{t}{\tau_1}\right)^{\beta_1}\right] + A_2 \exp\left[-\left(\frac{t}{\tau_2}\right)^{\beta_2}\right]. \quad (4)$$

$\tau_i$  are diffusion times for the first and second diffusion processes and  $\beta_i$  are the stretching parameters and their deviations from unity are a measure of the heterogeneity of the characterized systems or processes. The curves presented on Fig.3 are fitted using Microcal Origin software applying the Levenberg–Marquardt method to minimize the chi-square value.

The inset of Fig. 3 presents the plot of calculated diffusion time  $\tau_1$  as a function of the square of spots radius. It is seen that a very good linear dependence has been obtained. From the slope of the linear fit a diffusion constant value of  $4.2 \times 10^{-7}$  cm<sup>2</sup>/s was calculated. The calculated stretching parameters are  $\beta_1=1$  for the increase in the profile and  $\beta_2=0.8$  for the subsequent decrease indicating some heterogeneity of the second process.

### 3.2 Calculation of diffusion coefficient

The most important conclusion from Fig. 3 is that the post-exposure temporal growth of the surface profile is diffusion-determined process. Therefore it could be described by the widely used one-dimensional diffusion equation (See for example [8]):

$$\frac{\partial m(x,t)}{\partial t} = \frac{\partial}{\partial x} \left[ D(x,t) \frac{\partial m(x,t)}{\partial x} \right], \quad (5)$$

where  $m(x,t)$  is the monomer concentration,  $D(x,t)$  is the diffusion coefficient and  $t$  and  $x$  are the time and spatial coordinates. In Eq. (5) the term associated with the polymerization has

been omitted because we assumed that the polymerization stops shortly after exposure. Furthermore, because the growth of the profile is due to monomer diffusion, we can assume that the height of the profile  $h(x,t)$  is proportional to the monomer concentration:

$$h(x,t) \propto A(m(x,t) - m_0), \quad (6)$$

where  $m_0$  is the initial monomer concentration (spatially and time independent) and  $A$  is the proportionality constant. Eq. (6) is well understandable especially at the center of the spot where accumulation of monomer leads to swelling. Because  $h$  is measured in a small area around the center of the profile we can assume that  $D$  is spatially independent. Then Eq. (5) and Eq. (6) lead to:

$$\frac{\partial h(x,t)}{\partial t} = D(t) \frac{\partial^2 h(x,t)}{\partial x^2}, \quad (7)$$

Further, because spatial and time dependences of  $h$  are measured (Fig.2) we can calculate the partial derivatives in Eq. (7). The measured curves  $h(t)$  and  $h(x)$  were smoothed before the differentiation. A smooth curve  $h(t)$  was generated by fitting the experimental data using Eq. (4) as described above. The function,  $h(x)$ , was smoothed using the Microcal Origin FFT filter for curve smoothing. The first derivative of  $h$  with respect to the time  $t$  and the second derivative of  $h$  with respect to spatial coordinate  $x$  were calculated from the measured time (Fig. 2b) and spatial (Fig. 2a) dependences of the profile, respectively, by averaging the slopes of two adjacent data points using the Microcal Origin Program. The diffusion coefficient is calculated from:

$$D(t = t_i) = \left( \frac{\partial h}{\partial t} \Big|_{t=t_i, x=x_c} \right) / \left( \frac{\partial^2 h}{\partial x^2} \Big|_{t=t_i, x=x_c} \right), \quad (8)$$

where  $t_i = 15, 30, \dots, 300$ s and  $x_c$  is the centre of the profile.

In Eq. (7) we also assume that the movement of monomers is in the lateral direction only. To verify this, samples with different thicknesses were analysed. The results for their diffusion coefficients  $D$  are presented in Fig. 4.

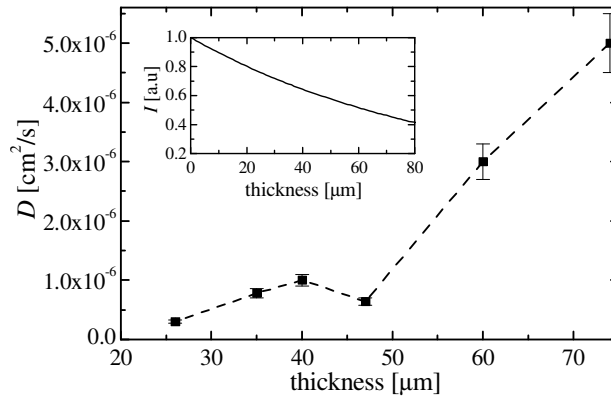


Fig. 4 Thickness dependence of diffusion coefficient and intensity dependence on depth (inset) for photopolymer layer;

It is seen that in the thickness range 30-50 $\mu$ m the diffusion coefficient is almost independent of the thickness as it should be expected if the model used to describe the observed swelling is valid, and then it increases with thickness. To clarify the thickness

dependence of  $D$ , the intensity attenuation through the layer was calculated and is presented as an inset in Fig. 4. The value of the absorption coefficient used in the calculation is firstly determined from transmittance and reflectance measurements of the sample. It is seen that for  $60\mu\text{m}$  thick layers the light intensity at the upper boundary is almost twice that at the lower. Having in mind that the polymerization rate increases with light intensity [8-11,22] it may happen that more monomer is polymerized nearer the surface than in the depth and, as a result, monomer mass-transport in the vertical direction can take place. In this case, Eq. (5) is no longer valid and two- or three-dimensional diffusion models should be used where diffusion in depth and attenuation of light inside the material are also considered [23,24].

It should be noted that all investigations presented here were carried out in layers about  $35\mu\text{m}$  thick thus ensuring that the monomer movement is in lateral direction only and the amount of monomer coming from the depth is negligible.

In order to estimate the accuracy, several measurements were conducted at different locations on the sample and  $D$  was calculated for each set of measurements. The obtained standard deviation from the mean value is less than 10%.

### 3.3 Intensity dependence of $D$

Fig. 5 presents the intensity dependence of diffusion coefficient for the two processes. The results show that the photopolymer permeability is influenced by the illuminating intensity. High values of diffusion coefficient are obtained for higher intensities.

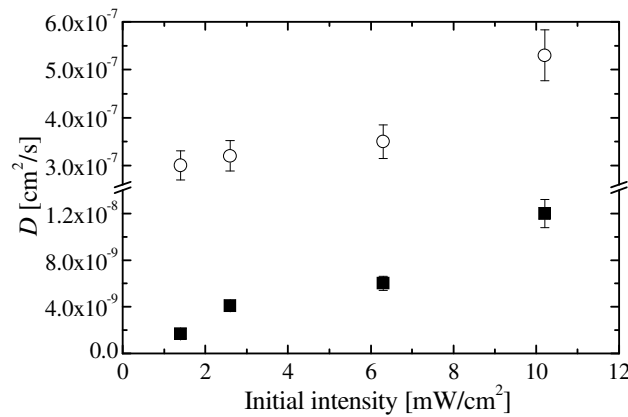


Fig. 5 Intensity dependence of diffusion coefficient for the first (open circles) and second (solid squares) diffusion processes. Some of the error bars are within the symbols. (initial time of illumination is 30s).

Considering that the polymerization rate increases with intensity [8-11,22], this behaviour of  $D$  is somewhat unexpected because if at higher intensity more polymer is formed, the density of the sample will increase and the diffusion will slow down. However, it has been established that higher intensity leads to the formation of shorter polymer chains [25]. Therefore, due to shorter polymer chains the sample illuminated at higher intensity could be less dense than a sample illuminated at lower intensity and the diffusion through it would be easier, that means the diffusion coefficient will be higher. A similar dependence of  $D$  on the intensity is observed for the second process (decrease in the profile height). Having in mind that usually it is assumed that this process is polymer diffusion away from the illuminated area, [12,13] the increase of  $D$  for higher intensity can be explained by greater mobility of the shorter polymer chains.

Another issue to be considered is the possible effect of increase of the temperature in the case of higher intensity illumination. It has been shown that if during recording the temperature increases by 10 degree, for example, this will lead to increase of diffusion coefficient by factor of two [26]. Hence, higher values of  $D$  for higher intensity can be expected, especially for the first process. However, 120 s after the initial illumination (the second process), the temperature dependence of  $D$  should be weaker than that for the first process and in fact no significant influence of the temperature on  $D$  should be observed. To the contrary, our experimental results showed that for the second process the intensity dependence of  $D$  is as pronounced as for the first process. This leads us to the conclusion that the first explanation of intensity dependence of  $D$  is more likely.

### 3.4 Polymer density dependence

The proposed method can be used for studying the density dependence of the diffusion coefficient. To do this we varied the illumination time from 15s to 60s keeping the intensity constant. By varying the illumination time we are able to simulate to some extent the polymer density change during real recording. Because the intensity is kept constant it is expected during longer illumination that more polymer will be formed. This will lead to an increase of the sample density and consequent decrease of diffusion coefficients for both processes. The confirmation of this assumption may be seen from Fig.6 which presents the calculated diffusion coefficients for the two processes.

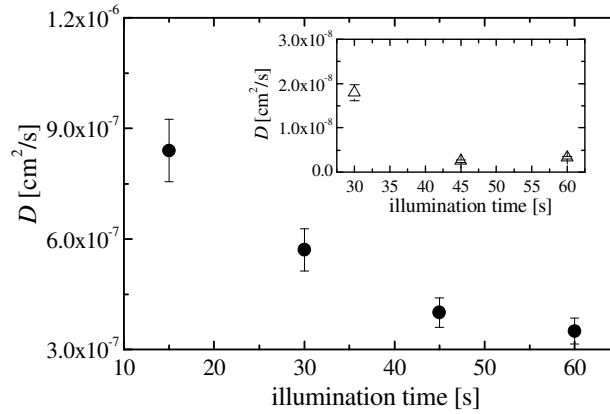


Fig. 6 Dependence of diffusion coefficient on the illumination time for the first and second (inset) process. (Intensity is 10 mW/cm<sup>2</sup>)

The dependence of diffusion coefficient on polymer (or monomer) concentration can be obtained in explicit form if the concentrations are determined for each illumination time from independent measurements. These measurements are in progress in our laboratory.

It should be noted here that a very good agreement between calculated values of  $D$  using Eq. (8) ( $D=5.3 \times 10^{-7}$  cm<sup>2</sup>/s) and the value from the slope of the curves of  $\tau$  vs  $r^2$  ( $D=4.2 \times 10^{-7}$  cm<sup>2</sup>/s) is obtained. Comparison with the values of monomer and polymer diffusion coefficients obtained from the post-exposure dynamics of the diffraction efficiencies of weak gratings [13] shows that Eq. (8) gives values about an order of magnitude higher. A possible reason may be that the method for calculation of  $D$  presented here gives near-surface values of  $D$  and some alteration of the surface may be expected compared to the volume. But we believe that the most probable reason of the observed discrepancies is the different wavelengths of initial illumination (554 nm in our study, compared to 532 nm in Ref. [13]). Even under the same conditions of initial exposure, the polymerization rates will be different

due to different absorption coefficients of the sensitizing dye at these two wavelengths. Consequently, the degree of conversion of monomer to polymer will not be the same. This problem could be overcome if a narrow band filter with central wavelength of 532nm is used instead of 554nm filter.

In this work we used poly(vinyl alcohol)-acrylamide photopolymer in order to demonstrate the applicability of the proposed method even in the case of a photopolymerisable system containing an immobile matrix that can impede the surface profile formation. But the use of the method is not restricted to photopolymer only. It can be applied for studying the diffusion process in all photosensitive system where surface relief profile is formed due to mass-transport of some species.

#### **4. Conclusions**

We have demonstrated a method for determination of diffusion coefficients of photopolymerisable systems that also provides a visualization of monomer mass-transport by a panoramic view over the studied surface. The method is based on the study of surface relief profile formation and evolution in a single illuminated spot using a commercially available White Light Interferometric surface profiler. It was shown that the observed swelling in the illuminated spot is due to diffusion of monomer from unexposed to exposed area driven by the concentration gradient set up by monomer polymerization. The determination of  $D$  is simple and straightforward; no complicated multiparametric models or nonlinear fitting procedures are needed. Moreover, the diffusion coefficient is determined separately from the polymerization rate, eliminating the necessity for preliminary information and assumptions in the modeling of processes taking place in holographic recording in photopolymers. The calculated values for the diffusion coefficients are in very good agreement with the values obtained from the slope of the linear dependence of diffusion time on distance squared. Furthermore very good reproducibility is achieved. By varying the conditions of initial exposure, polymer density and intensity dependence of  $D$  can be obtained. Despite the fact that the method gives the near-surface values of  $D$  it could be successfully applied for comparative studies and we believe it will be useful in material science.

#### **Acknowledgements**

This publication has emanated from research conducted with the financial support of Science Foundation Ireland.

The authors would like to acknowledge the School of Physics at DIT and Facility for Optical Characterisation and Spectroscopy, DIT for technical support

T. Babeva would like to thank the Arnold F. Graves Postdoctoral programme at DIT and Central Laboratory of Photoprocesses, Bulgarian Academy of Sciences.